J. Mol. Biol. (1993) **230**, 733–738

Double Strand Packing in Hemoglobin S Fibers

Isabelle Cretegny and Stuart J. Edelstein†

Department of Biochemistry, University of Geneva
CH-1211 Geneva 4, Switzerland

(Received 21 August 1992; accepted 22 December 1992)

The sickling variant of human hemoglobin, Hb S (β6 Glu→Val), assembles into 14-strand helical fibers composed of seven pairs of double strands. The organization of the helical double strands closely resembles the parallel, half-staggered, linear strand pairs of the crystals of Hb S characterized by Wishner *et al.* In the crystals, the molecules are arranged such that each possesses a β6 Val in contact with a molecule on the opposite strand. In the fibers, the overall hexagonal packing of strands leads to 22 classes of potential contacts between the seven double strands, but the presence of 2-fold helical symmetry reduces these contacts to 11 distinct classes. An analysis of the intermolecular contacts reported by Watowich *et al.*, based on the data of Carragher *et al.*, indicated a loosely packed structure for which only four of the 11 potential classes of contacts between double strands are significant (residues within 5 Å). We have recently analyzed the packing based on the results of Dykes *et al.* and Rodgers *et al.*, and compared the findings with the structure derived from the data of Carragher *et al.* We find serious differences between the two data sets concerning the packing of double strands. The Dykes–Rodgers data indicate a more closely packed structure in which nine of the 11 potential classes of contacts are within 5 Å. Considerations on the stability of certain contacts derived from incomplete fibers, as well as studies of Hb molecules composed of β^S chains and mutant α chains, suggest that the structural model with closer packing of the double strands provides a better correlation with the other experimental results.

Keywords: molecular modeling; intermolecular contacts

Although the sickling variant of hemoglobin (Hb S) arises from a single amino acid substitution, β6 Glu→Val (Ingram, 1956), the polymerization of Hb S molecules into fibers is an exceedingly complex process, both from the structural and kinetic points of view (Eaton & Hofrichter, 1990). The basic fiber structure, determined by Dykes *et al.* (1978) from electron microscope data and image reconstruction, is composed of 14 helical strands of Hb S molecules, with a core of four inner strands surrounded by ten external strands, arranged in an elliptical cross-section. Subsequent studies on incomplete fibers lacking pairs of strands led to the proposal that the fibers are organized in terms of seven half-staggered double strands (Dykes *et al.*, 1979), with molecules within each double strand arranged in a manner similar to the half-staggered double strands in the crystals of Hb S studied by Wishner *et al.* (1975). The pairing scheme was subsequently confirmed by direct analysis of fiber cross-sections from electron microscope data (Rodgers *et al.*, 1987). This latter study also determined the polarity of the double strands, revealing that the four outermost pairs are of opposite polarity to the three other pairs. Apart from the central pair, the other six pairs of double strands occur in three symmetry-related sets.

Conflicting models for the Hb S fiber structure were proposed by other groups, based on 16 strands (Wellems & Josephs, 1979; Wellems *et al.*, 1981; Potel *et al.*, 1984) or alternative pairing schemes (Magdoff-Fairchild *et al.*, 1982; Rosen & Magdoff-Fairchild, 1988), but one of these groups subsequently confirmed the 14-strand model, including the pairing and polarities of double strands (Carragher *et al.*, 1988). Based on their results, molecular modeling was carried out on the Hb S fiber structure in order to characterize the intermolecular contacts (Watowich *et al.*, 1989). As reported here, we have recently completed a similar molecular modeling study in which we compared the results obtained with the Dykes–Rodgers structural data (Dykes *et al.*, 1979; Rodgers *et al.*, 1987)

† Author to whom all correspondence should be addressed at: Department of Biochemistry, University of Geneva, 30 Quai Ernest Ansermet, CH-1211 Geneva 4, Switzerland.

0022–2836/93/070733–06 $08.00/0

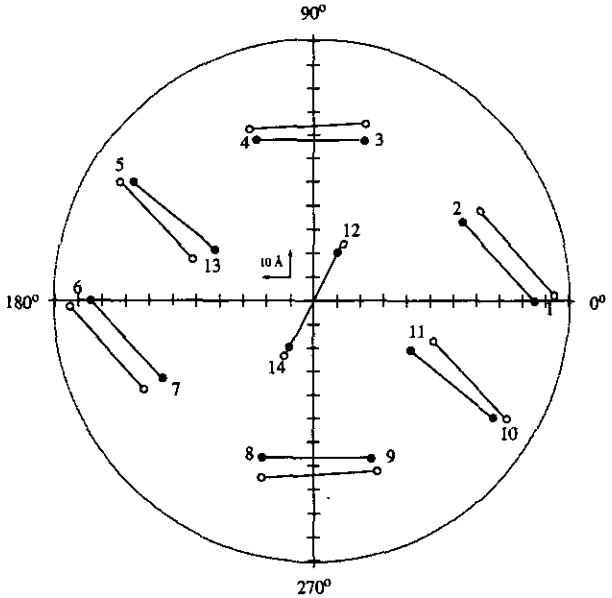

Figure 1. Cross-sectional projection of the placement of strands for the 2 data sets examined. The Dykes–Rodgers strand positions (Dykes *et al.*, 1979) are presented as filled circles; the Carragher strand positions (Carragher *et al.*, 1988) are presented as open circles. For both data sets, strands belonging to "double strands" (Wishner *et al.*, 1975) are connected by lines. The 2 data sets were centered and aligned along the axis between strands 12 and 14. The hatch marks along the ordinate and the abscissa are spaced at 10 Å intervals. Concerning the third dimension, *Z* (displacement along the fiber axis), the 2 data sets give the following results (where the Dykes–Rodgers data are presented for each strand, with the position for strand 1 set as zero, with the relative displacement for each successive strand given in Å, and with the displacement that must be applied to reproduce the Carragher data presented in parentheses): strand 1, 0·0 Å (+2·6 Å); strand 2, 32·0 Å (+2·6 Å); strand 3, 51·2 Å (+0·1 Å); strand 4, 19·2 Å (+0·1 Å); strand 5, 44·4 Å (−1·8 Å); strand 6, 32·0 Å (+2·2 Å); strand 7, 0·0 Å (+3·0 Å); strand 8, 19·2 Å (+0·5 Å); strand 9, 51·2 Å (+0·3 Å); strand 10, 12.4 Å (−1.4 Å); strand 11, 44·4 Å (−1·8 Å); strand 12, 0·0 Å (−2·1 Å); strand 13, 12·4 Å (−1·4 Å); strand 14, 32·0 Å (−2·5 Å). The Dykes–Rodgers data set was derived from the surface lattice of Fig. 9 of the original article by Dykes *et al.* (1979), with the axial displacement (*Z*) of the strands belonging to pairs adjusted to incorporate the subsequent refinements presented by Rodgers *et al.* (1987), so as to coincide with the 32 Å displacement within double strands. In addition, a scaling factor was applied to the Dykes–Rodgers data to take into account the fact that the surface lattice was originally constructed on a spacing of 30 Å, rather than the 32 Å displacement, corresponding to the crystal lattice (Wishner *et al.*, 1975). The Carragher data were derived from Table 3 of their article (Carragher *et al.*, 1988), with the addition of minus signs to the *Z* values of strands 3 and 4 and the *Y* value of strand 14, in order to correct for an erratum of publication that was confirmed by R. Josephs (personal communication).

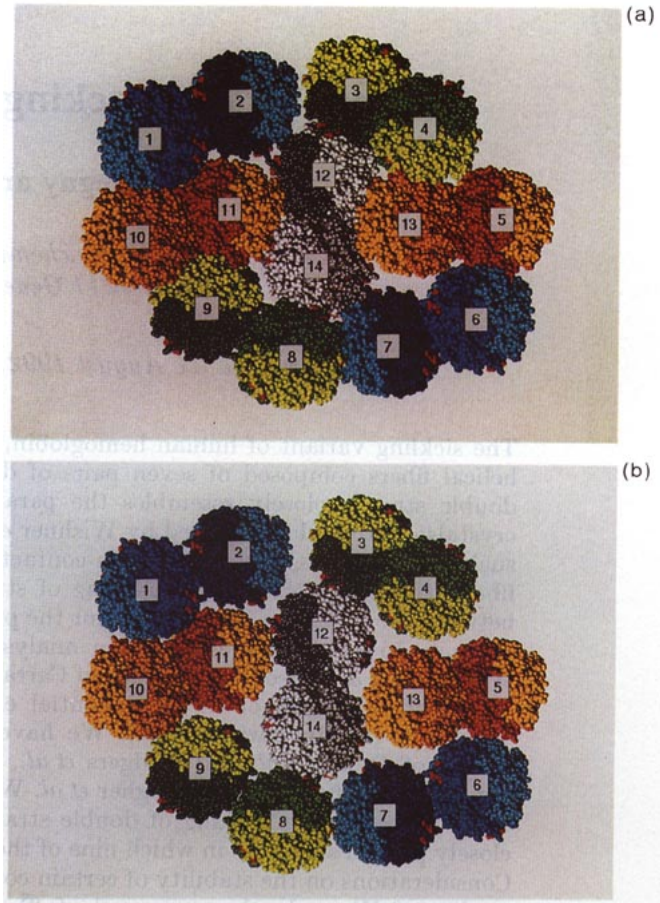

Figure 2. Molecular model of double strand packing of Hb S fibers. A cross-section of the fiber is presented with 1 molecule for each strand with the Dykes–Rodgers data set (in A) and the Carragher data set (in B), using the same scale for both representations. The molecules, obtained with the co-ordinates of Padlan & Love (1985) deposited in the Brookhaven Data Bank (accession number 1hbs.pdb), are arranged as defined in Fig. 1, but viewed from the opposite direction. Therefore the order of the strands is clockwise, rather than counter-clockwise as in Fig. 1. For each model, the strands are arranged to include the helical transition from linearity by a rotation of 7·8°/64 Å and the appropriate angle with respect to *Z* to account for the helical path of the strand. Symmetry-related double strands are presented with the same colors; for each molecule the β chains are darker than the α chains and for the two molecules of each double strand, the molecule farther into the plane of the figure is additionally darkened. Heme atoms are presented in red. Apparent spacing differences in projection between symmetry-related strands, e.g. 2–3 and 7–8, are due to the helical twist coupled with differences in position along the *Z* axis. For example, in the arrangements presented, the Hb molecule of strand 8 is "above" the Hb molecule of strand 7, whereas for the symmetry-related contact the Hb molecule of strand 3 is "below" the Hb molecule of strand 2.

and with the Carragher structural data (Carragher *et al.*, 1988).

Although the Carragher and Dykes–Rodgers structural models for the Hb S fibers are similar in terms of the basic pattern of helical organization, the distances between strands vary considerably in the two cases. From the comparison presented in Figure 1, it can be observed that the positions for the individual strands in the two models lie along

Table 1
Contacts within 5 Å between double strands

Contact		Z value	Closest residues		Carragher contact
1–10	[6–5]	+Z	$\alpha_2$72 His	$\beta_2$87 Thr	+
1–11	[6–13]	+Z	$\alpha_2$53 Ala	$\beta_1$58 Pro	
2–3	[7–8]	−Z	$\alpha_1$60 Lys	$\alpha_1$51 Gly	
2–11	[7–13]		(none within 5 Å)		+
2–12	[7–14]	+Z	$\beta_2$59 Lys	$\beta_2$59 Lys	
2–12	[7–14]	−Z	$\alpha_1$47 Asp	$\alpha_1$54 Gln	
3–12	[8–14]	+Z	$\beta_2$87 Thr	$\alpha_2$4 Pro	+
4–5	[9–10]	−Z	$\alpha_2$4 Pro	$\alpha_2$54 Gln	
4–12	[9–14]		(none within 5 Å)		
4–13	[9–11]	−Z	$\alpha_1$4 Pro	$\beta_2$76 Ala	
11–12	[13–14]	+Z	$\alpha_1$18 Gly	$\beta_1$5 Pro	+
11–14	[13–12]	+Z	$\beta_1$54 Gln	$\alpha_2$80 Lys	

The contacts are designated between strands as numbered in Fig. . For each contact attributed with the Dykes–Rodgers data (atoms within 5 Å), the *Z* value (position along the *Z* axis) indicates whether the molecule in the second strand is above (+*Z*) or below (−*Z*) the molecule in the first strand, e.g. for the contact 1–10 (or 6–5) +*Z* indicates that the molecule of strand 10 (or 5) is at a higher *Z* value than the molecule of strand 1 (or 6). The nearest residues indicate the point of closest contact between the 2 strands of the contacts, e.g. for the contact 1–10, the $\alpha_2$72 His is on strand 1 and the $\beta_2$87 Thr on strand 10. The subscripts refer to the orientation of the β-6 Val at the contact that defines subunit β_2, as well as α_2 on the same α–β dimer. A plus (+) sign in the last column indicates that a contact between strands was reported by Watowich *et al.* (1989) based on the Carragher parameters.

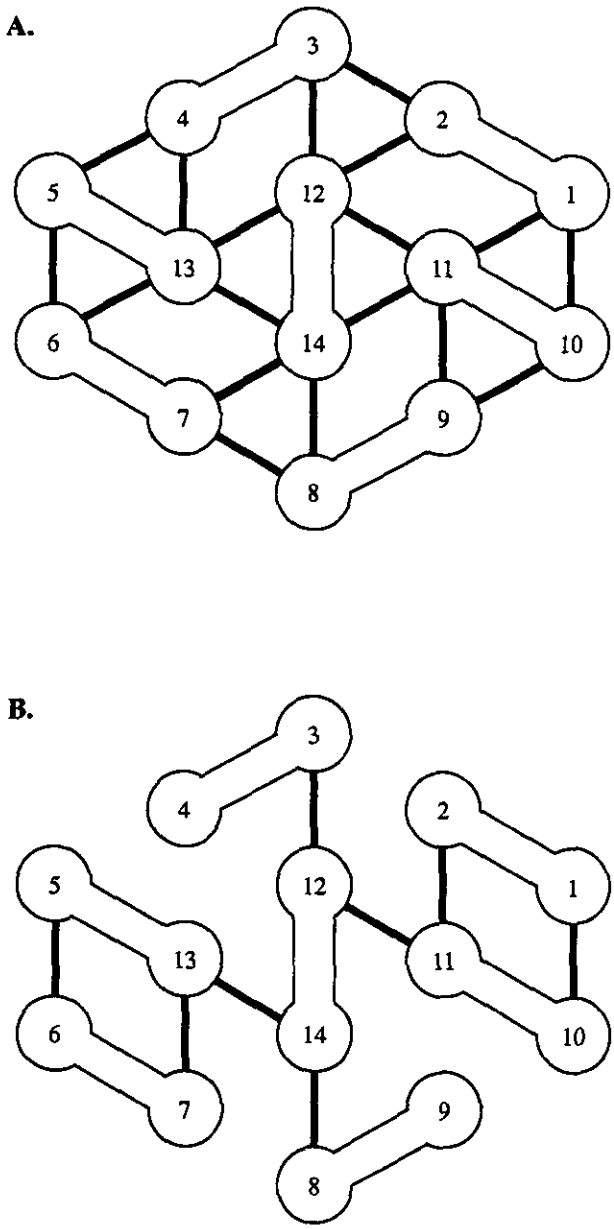

Figure 3. A representation of the presence or absence of contacts between double strands for the data sets of Dykes–Rodgers (in A) and Carragher (in B).

near y identical radial lines, but in every case the positions in the Dykes–Rodgers model are closer to the center. The largest difference occurs for the outermost strands (1 and 6), which in the Carragher model are placed with their centers at a radius about 10 Å greater than in the Dykes–Rodgers model (1 Å = 0·1 nm). Some differences between the two models also exist for the displacements of the molecules of each strand along Z, the fiber axis, (see legend to Figure 1), but the differences in *Z* are smaller (an average of 1·6 Å) than the radial differences.

When the differences in radial placement of the strands are compared at the level of the molecular models, as presented in Figure 2, it is clear that the greater radial distances for the Carragher data result in far fewer contacts between double strands than for the Dykes–Rodgers data. On the basis of the Carragher data, Watowich *et al.* (1989) identified intermolecular contacts between double strands (residues within 5 Å) for only four of the 11 potential classes of contacts, whereas the model generated with the Dykes–Rodgers data (Table 1) indicates interactions for nine of the 11 possible contact classes. Of these nine contacts observed with the Dykes–Rodgers positions, three were also reported by Watowich *et al.* (1989) with the Carragher positions. However, the fourth contact of Watowich *et al.* (1989) between strands 2 and 11 (or 7 and 13), was not observed with the Dykes–Rodgers data.

For the nine Dykes–Rodgers contacts described in Table 1, the interaction is between a molecule of the first strand with a molecule at either a higher or lower *Z* value, except for the contact 2–12 (or 7–14) for which the molecules implicated are effectively "half-staggered" and interact at both higher and lower *Z*. The presence or absence of contacts between the various double strands with the Dykes–Rodgers or Carragher data are summarized in Figure 3A and B, respectively.

The involvement of only four classes of contacts between double strands as proposed by Watowich *et al.* (1989) on the basis of the Carragher data is not readily reconciled with other experimental results. For example, in certain incomplete fibers (Dykes *et al.*, 1979) or fibers obtained with the double mutant, Hb S-Sealy, composed of β chains from Hb S and α chains from Hb Sealy (Crepeau *et al.*, 1981), the

Table 2

Participation at contacts between double strands of sites of single amino acid substitutions of mutant hemoglobins that alter polymerization

Variant	Substitution	Dykes–Rodgers contact	Watowich contact
Sawara	α6 Asp→Ala	3–12, 4–13	Not found
Antharaj	α11 Lys→Glu	1–10, 2–3, 3–12	Not found
Sealy	α47 Asp→His	2–3, 2–12, 4–5, 11–14	+
J Mexico	α54 Gln→Glu	2–3, 2–12, 4–5, 11–14	+
G Philadelphia	α68 Asn→Lys	1–10, 2–3	+
Winnipeg	α75 Asp→Tyr	1–10, 3–12, 11–12	+
Stanleyville-II	α78 Asn→Lys	1–10, 3–12, 4–13, 11–12	+
Detroit	β95 Lys→Asn	11–14	+
N Baltimore	β95 Lys→Glu	11–14	+

The compilation presented here is limited to mutation sites of hemoglobin that were listed in Table 1 of the article by Watowich *et al.* (1989) as affecting gelation, but not found at contacts (axial or lateral) within double strands.

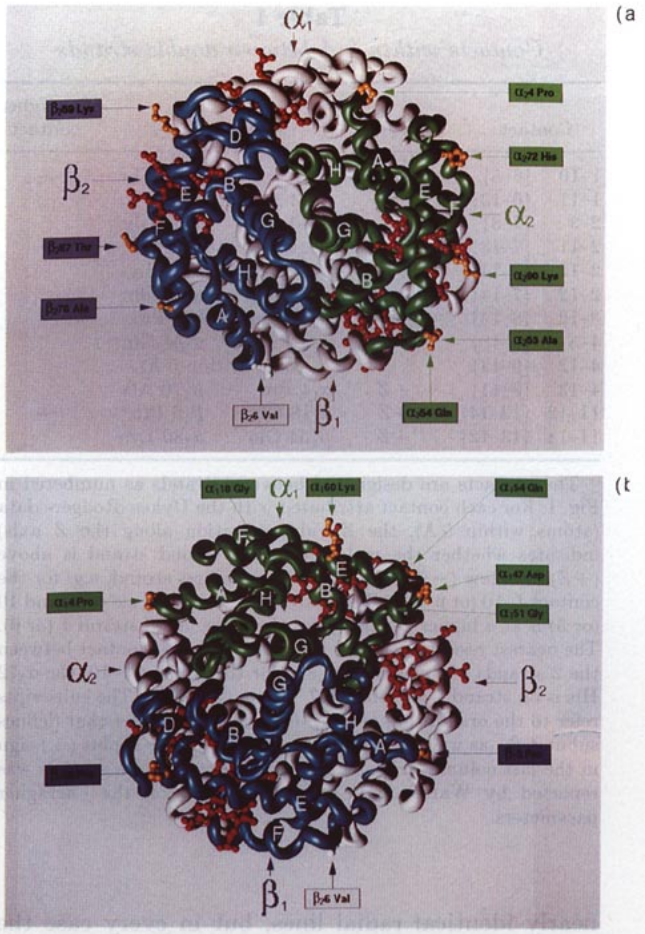

Figure 4. Placement of the residues participating in contacts between double strands. Two views of the helical backbone of the hemoglobin molecule are presented (A and B) corresponding to a rotation of 180°. In A, residues at the center of contacts between double strands present on the same α–β dimer that contributes the $\beta_2$6 Val to the lateral contact are indicated in color (green for α chains; blue for β chains), whereas for the other α–β dimer the backbone is depicted in gray (the heme molecules are in red for all 4 subunits). In B the pattern is reversed, with the α–β dimer that does not possess the β6 Val at the lateral contact presented in color, along with the residues within this dimer that participate at contacts between double strands. Sides-chains of the residues at contacts between double strands noted in A and B are orange. The contacts at which the various residues indicated participate are given in Table 1.

double strands 1–2 (and the equivalent 6–7) are lost, suggesting that the contacts linking these double strands to the other strands are relatively weak. However, Watowich *et al.* (1989) assign two of their four classes of contacts to these double strands. While the presence of a contact does not provide a direct indication of its strength (it could in fact be repulsive), if half of the contacts involve the two strand pairs most readily dissociated, the other two sets of contacts must be sufficient to stabilize the remainder of the structure.

The results with the double mutant Hb S-Sealy are also informative with respect to contact assignment, since the position mutated in Hb Sealy, α47 Asp→His, is found to lie at the center of the contact 2–12 with the Dykes–Rodgers data, whereas this contact is not observed with the Carragher data (Table 1). Correlations with altered fiber stability of molecules composed of β^S chains and mutated α chains, such as from Hb Sawara and Hb Antharaj with substitutions at the residues α6 and α11, respectively (Benesch *et al.*, 1979), provide additional information, since these sites were not found at the contacts described by Watowich *et al.* (1989) with the Carragher data, but with the Dykes–Rodgers data the sites are present at contacts between double strands (Table 2). Other α chain mutants that influence fiber formation (Benesch *et al.*, 1977) and were found at contacts between double strands by Watowich *et al.* (1989) also occur at contacts between double strands with the Dykes–Rodgers data, as summarized in Table 2.

In terms of overall packing, the four-strand complexes ((1–2)(10–11)), or the equivalent ((6–7)(5–13)), are each linked to the rest of the fiber structure according to the Carragher data by only one contact (see Fig. 3), between strands 11 and 12 (or between strands 13 and 14). It is questionable whether sufficient fiber stability is plausible with so few interactions. In contrast, the Dykes–Rodgers data result in six contacts between each of these four-strand bundles and the adjacent strands (Fig. 3). More precise estimates of contact strengths would require energy calculations, but at the current level of analysis, the molecular positions are not sufficiently accurate to warrant minimizations or molecular dynamics simulations to estimate free energy values for the contacts between double strands. Within double strands, calculations have been carried out for the primary β6 site (Kuczera *et al.*, 1990; Schaad, 1991) and site-directed mutagenesis has also been applied to characterize this site

(Baudin-Chich *et al.*, 1990; Bihoreau *et al.*, 1992). This latter approach could also provide valuable information on the contacts between double strands. The positions of the residues that contribute to the nine classes of contacts with the Dykes–Rodgers data are indicated on a representation of the hemoglobin molecule in Figure 4.

Overall, the Dykes-Rodgers data would appear to provide a more consistent model of double strand packing than the Carragher data. The differences arise principally as a result of the placement of the strands so far apart in the Carragher model that many of the potential contacts cannot occur (Fig. 1). Small differences in Z between the two data sets also exist (see legend to Fig. 1), but changes in Z could not compensate for the failure to achieve contacts due to radial distances. The origin of the differences in radial positions for the Dykes–Rodgers and Carragher data sets does not appear to involve sample preparations, but may result from a failure of Carragher *et al.* (1988) to compensate for fiber flattening on the electron microscope grids. Dykes *et al.* (1979), from measurements on tilted samples, reported a 15% correction for flattening that reduced the values for the wide and narrow diameters from 270 Å to 230 Å and from 210 Å to 180 Å, respectively. The lower values are in general agreement with the observations for average fiber diameters in embedded cells (Crepeau *et al.*, 1978), although packing differences involving the orientation with respect to wide and narrow diameters complicate direct observations on cross-sections (Garrel *et al.*, 1979; Edelstein & Crepeau, 1979; Rodgers, 1987; McDade *et al.*, 1989). In contrast, the values of the Carragher group, 250 Å and 185 Å (McDade *et al.*, 1989), are suggestive that the wide diameter has been significantly overestimated. The narrow diameter reported by McDade *et al.* (1989), 185 Å, is close to the value of 180 Å reported by Dykes *et al.* (1979), but the strand positions (Fig. 1) based on Table 3 of Carragher *et al.* (1988) correspond to a diameter of about 200 Å, which would suggest that the narrow diameter has also been overestimated.

Apart from uncertainties due to flattening, the positions of molecules derived from the electron microscope data were estimated to possess an uncertainty of 2 Å (Dykes *et al.*, 1979). Within these limits, the presence of specific residues at the different classes of contacts identified between double strands with the Dykes–Rodgers data can be assigned with reasonable confidence, although for several of the contacts presented in Table 1 some minor overlapping of atoms occurs. The overlaps could be eliminated by minimization, but with uncertainties of up to 2 Å in the placement of molecules, the distances are not sufficiently exact to justify detailed energy refinements. Therefore, before attempting more complicated analyses of the contacts, it would be preferable to obtain improved data on the locations of molecules, as might be derived from X-ray diffraction measurements (Magdoff-Fairchild *et al.*, 1972; Rodgers *et al.*, 1986; Rosen & Magdoff-Fairchild, 1988) and efforts along these lines are being pursued. Cryo-electron microscopy could also be employed to obtain improved data on molecular positions within the fibers.

This work was supported by a grant from the Swiss National Science Foundation. We thank Edouard de Castro and Peter Flükiger for their help with computational problems and Drs M. Rozycki and D. Pascolini for valuable comments on the manuscript.

References

Baudin-Chich, V., Pagnier, J., Marden, M., Bohn, B., Lacaze, N., Kister, J., Schaad, O., Edelstein, S. J. & Poyart, C. (1990). Enhanced polymerization of recombinant human deoxyhemoglobin β6 Glu→Ile. *Proc. Nat. Acad. Sci., U.S.A.* **87**, 1845–1849.

Benesch, R. E., Kwong, S., Benesch, R. & Edalji, R. (1977). Location and bond type of intermolecular contacts in the polymerization of haemoglobin S. *Nature (London)*, **269**, 772–775.

Benesch, R. E., Kwong, S., Edalji, R. & Benesch, R. (1979). α Chain mutations with opposite effects on the gelation of hemoglobin S. *J. Biol. Chem.* **254**, 8169–8172.

Bihoreau, M. T., Baudin, V., Marden, M., Lacaze, N., Bohn, B., Kister, J., Schaad, O., Dumoulin, A., Edelstein, S. J., Poyart, C. & Pagnier, J. (1992). Steric and hydrophobic determinants of the solubilities of recombinant sickle cell hemoglobin. *Protein Sci.* **1**, 145–150.

Carragher, B., Bluemke, D. A., Gabriel, B., Potel, M. J. & Josephs, R. (1988). Structural analysis of polymers of sickle cell hemoglobin. I. Sickle hemoglobin fibers. *J. Mol. Biol.* **199**, 315–331.

Crepeau, R. H., Dykes, G., Garrell, R. & Edelstein, S. J. (1978). Diameter of haemoglobin S fibres in sickled cells. *Nature (London)*, **274**, 616–617.

Crepeau, R. H., Edelstein, S. J., Szalay, M., Benesch, R. E., Benesch, R., Kwong, R. & Edalji, R. (1981). Sickle cell hemoglobin fiber structure altered by α-chain mutation. *Proc. Nat. Acad. Sci., U.S.A.* **78**, 1406–1410.

Dykes, G., Crepeau, R. H. & Edelstein, S. J. (1978). Three-dimensional reconstruction of the fibers of sickle cell hemoglobin. *Nature (London)*, **272**, 506–510.

Dykes, G., Crepeau, R. H. & Edelstein, S. J. (1979). Three-dimensional reconstruction of the 14-filament fibers of hemoglobin S. *J. Mol. Biol.* **130**, 451–472.

Eaton, W. A. & Hofrichter, J. (1990). Sickle cell hemoglobin polymerization. *Advan. Protein Chem.* **40**, 63–279.

Edelstein, S. J. (1981). Molecular topology in crystals and fibers of hemoglobin S. *J. Mol. Biol.* **150**, 557–575.

Edelstein, S. J. & Crepeau, R. H. (1979). Oblique alignment of hemoglobin S fibers in sickled cells. *J. Mol. Biol.* **134**, 851–855.

Garrell, R. L., Crepeau, R. H. & Edelstein, S. J. (1979). Cross-sectional views of hemoglobin S fibers by electron microscopy and computer modeling. *Proc. Nat. Acad. Sci., U.S.A.* **76**, 1140–1144.

Ingram, V. M. (1956). A specific chemical difference between the globins of normal human and sickle-cell anemia haemoglobin. *Nature (London)*, **178**, 792–794.

Kuczera, K., Gao, J., Tidor, B. & Karplus, M. (1990). Free energy of sickling: A simulation analysis. *Proc. Nat. Acad. Sci., U.S.A.* **87**, 8481–8485.

Magdoff-Fairchild, B., Swerdlow, P. H. & Bertles, J. F. (1972). Intermolecular organization of deoxygenated sickle haemoglobin determined by X-ray diffraction. *Nature (London)*, **239**, 217–218.

Magdoff-Fairchild, B., Rosen, L. S. & Chiu, C. C. (1982). Triclinic crystals associated with fibers of deoxygenated sickle hemoglobin. *EMBO J.* **1**, 121–126.

McDade, W. A., Carragher, B., Miller, C. A. & Josephs, R. (1989). On the assembly of sickle hemoglobin fascicles. *J. Mol. Biol.* **206**, 637–639.

Padlan, E. A. & Love, W. E. (1985). Refined crystal structure of deoxyhemoglobin S. I. Restrained least-squares refinement at 3·0- Å resolution. *J. Biol. Chem.* **260**, 8272–8279.

Potel, M. J., Wellems, T. E., Vasser, D. J., Deer, B. & Josephs, R. (1984). Macrofiber structure and the dynamics of sickle cell hemoglobin crystallization. *J. Mol. Biol.* **177**, 819–839.

Rodgers, D. W. (1987). Sickle cell hemoglobin fibers: structural studies by electron microscopy and image reconstruction. Ph.D. thesis, Cornell University.

Rodgers, D. W., Crepeau, R. H. & Edelstein, S. J. (1986). Fibers of hemoglobin S: strand pairing and polarity. In *Approaches to the Therapy of Sickle Cell Anemia* (Beuzard, S., Charache, S. & Galacteros, F., eds), pp. 21–38, INSERM, Paris.

Rodgers, D. W., Crepeau, R. H. & Edelstein, S. J. (1987). Pairings and polarities of the 14 strands in sickle cell hemoglobin fibers. *Proc. Nat. Acad. Sci., U.S.A.* **84**, 6157–6161.

Rosen, L. S. & Magdoff-Fairchild, B. (1988). X-ray diffraction studies of 14-filament models of deoxygenated sickle cell hemoglobin fibers. II. Models based on the deoxygenated sickle hemoglobin crystal structure. *J. Mol. Biol.* **200**, 141–150.

Schaad, O. (1991). Modélisation moléculaire de deux protéines des globules rouges humains: l'hémoglobine et la bisphosphoglycerate mutase. Ph.D. thesis, University of Geneva.

Watowich, S. J., Gross, L. J. & Josephs, R. (1989). Intermolecular contacts within sickle cell hemoglobin fibers. *J. Mol. Biol.* **209**, 821–828.

Wellems, T. E. & Josephs, R. (1979). Crystallization of deoxyhemoglobin S by fiber alignment and fusion. *J. Mol. Biol.* **135**, 651–674.

Wellems, T. E., Vassar, R. J. & Josephs, R. (1981). Polymorphic assemblies of double strands of sickle cell hemoglobin. Manifold pathways of deoxyhemoglobin S crystallization. *J. Mol. Biol.* **153**, 1011–1026.

Wishner, B. C., Ward, K. B., Lattman, E. E. & Love, W. E. (1975). Crystal structure of sickle-cell deoxyhemoglobin at 5 Å resolution. *J. Mol. Biol.* **8**, 179–194.

Edited by A. Klug